

CHAPTER - IVWALLACE CORRECTED HHOB APPROXIMATION4.1 INTRODUCTION

Due to the recent advances both theoretical and experimental - in the study of electron scattering by atoms, the search for computationally feasible as well as accurate theoretical methods has been enhanced. But it is rather strange that none of the theoretical approximations explain equally successfully all the observed phenomena in scattering problems. Hence the theoretical physicist resorts to a particular method which applies best to the problem under consideration. With the introduction of certain modifications, the range of applicability of the method can be widened. In certain cases it is even found that simple modifications in a particular approximation improve the results tremendously. But sometimes it may happen that certain highly sophisticated calculations come out with poorer results than those of simpler approximations. In such cases, there might be some conspiracy of cancellation amongst the effects neglected by these simpler approximations. There is a lot of scope for the modifications of some of the commonly used approximations such that their validity criteria are

relaxed resulting in a wider range of applicability of the method. In the present chapter we have applied the Wallace type of trajectory corrections to the HHOB approximation proposed by Yates (1979).

The HHOB approximation proposed by Yates has several attractive features. The expressions for scattering amplitudes can be obtained in a closed form, thus avoiding the complex numerical procedures. The problem of divergent integrals (like those in GES) is absent and the method as such is simple and computationally easier. In the HHOB approximation the second Born term is handled in the same manner as the glauber approximation. At high energy the target is approximated as being frozen. The potential experienced by the incident particle will depend on the co-ordinate \underline{z} of the target particles. Since the projectile wave is approximated by straight line rays passing through a set of immobile particles in the second Born approximation, the phase shift of the projectile wave is the sum of phase shifts from interaction of each target particles. One can obtain the amplitude factor from the phase shifts. The second Born term treated in the Glauber way thus becomes very attractive.

In principle HHOB approximation is very well founded for a small angle scattering. At large

angle there is a considerable departure (Rao and Desai 1981, 83). Hence it was desirable to try certain modifications on this approximation such that better results can be expected out of the application of the improved methods. The Chief motivation behind such an idea is the work reported by Wallace (1973) who used a technique introduced by Abarbanel and Itzkson to obtain the leading corrections to the eikonal amplitude. He has incorporated the trajectory correction in the expansion of the Green's function of the eikonal approximation and carried out further analysis of the perturbation series. However the resulting many body Wallace amplitude does not eliminate all the difficulties inherent in the Glauber amplitude. In particular, the Wallace extension of the Glauber approximation is still a zero excitation energy approximation and therefore does not account for long range polarisation effects at small angles and represent inadequately absorption effects in the same region. As mentioned earlier, the similarity between the modes of expansion of the Green's function in the eikonal and HHOB approximation also. Keeping this in mind, in the present study, the HHOB analysis was carried out after incorporating the correction in the Green's function, the scattering amplitudes derived accordingly.

In this chapter we present a detailed study of the Wallace corrected HHOB approximation for electron-atom collisions. We have then applied this method to find out the DCS of electron-hydrogen, electron-helium and electron-lithium scattering in the energy range 100 eV to 400 eV. The total cross-section for hydrogen and lithium are also calculated for the energy range 100 eV to 400 eV and 100 eV to 1000 eV respectively. These are then compared with other recent calculations and experimental data.

4.2 THEORY

The T matrix for an elastic scattering process in Second Born approximation can be written as

$$T = \langle \psi_f | (V + V G_0 V) | \psi_i \rangle, \quad (4.1)$$

Where V is the interaction potential and G_0 is the particle propagator and is given by

$$G_0 = \sum_n \int \frac{dk}{k^2} \frac{|\psi_n\rangle \langle \psi_n|}{\frac{k_i}{2} - \epsilon_0 - \frac{k}{2} - \epsilon_n + i\epsilon} \quad (4.2)$$

The wave functions $|\psi_i(r_o, r_j)\rangle$ and $|\psi_f(r_o, r_j)\rangle$ are given by

$$\begin{aligned} |\psi_i\rangle &= (2\pi)^{-3/2} e^{i\mathbf{k}_i \cdot \underline{x}} \phi_i(\underline{x}_j), \\ |\psi_f\rangle &= (2\pi)^{-3/2} e^{i\mathbf{k}_f \cdot \underline{x}} \phi_f(\underline{x}_j), \end{aligned} \quad (4.3)$$

where \mathbf{k}_i and \mathbf{k}_f are the initial and final wavevectors for the incident and scattered particle, and ϕ_i and ϕ_f are the wave functions for target in the initial state and final state. The inverse of the operator G_0 is $G_0^{-1} = \frac{\mathbf{K}^2}{2} - \frac{\mathbf{P}^2}{2} - V + i\eta$ (4.4)

Expanding the momentum \mathbf{P} about the vector \mathbf{k}_n and neglecting the square term we will have the approximate eikonal approximation of G_0^{-1} ,

$$g^{-1} = \mathbf{v} \cdot (\mathbf{K} - \mathbf{P}) - V + i\eta \quad (4.5)$$

where \mathbf{v} is the velocity in the z direction.

$$\underline{k} = 1/2 (\underline{k}_i + \underline{k}_f)$$

The approximate T matrix can be obtained by the use of g in place of G_0 in (4.1)

$$T^0 = \langle \psi_f | v | \phi_i^+ \rangle = \langle \phi_f^- | v | \psi_i \rangle \quad (4.6)$$

where $|\phi_i^+\rangle$ and $|\phi_f^-\rangle$ used here satisfy the Lippmann-Schwinger equation with eikonal propagator g

used in place of the exact propagator G_0 . In the co-ordinate representation of these wave vectors we have

$$\begin{aligned} \phi_i^{(+)}(\underline{r}_0, \underline{r}_1) &= (2\pi)^{-3/2} [1 - \frac{i}{2k_n} \sum_n \\ &\quad \int_{-\infty}^z e^{-i\beta_{in} z'_0} v(x_0, y_0, z_0 - z'_0, \underline{r}_1) \\ dz'_0 | \phi_n(\underline{r}_j) &>] e^{ik_i \cdot \underline{r}_0} \\ &= (2\pi)^{-3/2} e^{ik_i \cdot \underline{r}_0} e^{i X_+} \end{aligned} \quad (4.7)$$

and

$$\begin{aligned} \phi_f^{*(-)}(\underline{r}_0, \underline{r}_1) &= (2\pi)^{-3/2} e^{-ik_f \cdot \underline{r}} [1 - \frac{i}{2k_i} \sum_n \\ &\quad \int_z^\infty e^{-i\beta_{in} z'_0} v(\underline{r}_0, y_0, z_0 - z'_0, \underline{r}_1) \\ dz'_0 | \phi_n(\underline{r}_j) &>] e^{-ik_f \cdot \underline{r}} e^{i X_-} \\ &= (2\pi)^{-3/2} e^{-ik_f \cdot \underline{r}} e^{i X_-} \end{aligned} \quad (4.8)$$

where $\beta_{in} = \Delta E/k_i$, ΔE is the excitation energy of the target.

Hence T^0 can be written as

$$\begin{aligned}
 T^0 &= (2\pi)^{-3} \langle \phi_i | \int e^{i\frac{q \cdot r}{\hbar}} dv V [1 - \frac{i}{2k_n} \sum_n \\
 &\quad \int_{-\infty}^z e^{-i\beta_{in} z_0'} v(x_0, y_0, z_0 - z_0', r_0) dz_0' | \phi_n \rangle \\
 &\quad \langle \phi_n | e^{ik_i, r_0} | \phi_i \rangle \\
 &= (2\pi)^{-3} \langle \phi_i | \int e^{i\frac{q \cdot r}{\hbar}} e^{iX_\pm} dv | \phi_i \rangle \quad (4.9)
 \end{aligned}$$

The Schrödinger equation $\frac{-1}{\hbar^2} \Psi(\underline{r}) = 0$ allows us to write

$$\int dz V(r) e^{iX_\pm} = v_i [e^{iX_0(b)} - 1] \quad (4.10)$$

$$\begin{aligned}
 \text{where } e^{iX_0(b)} &= [1 - \frac{i}{2k_n} \sum_n \int_{-\infty}^{\infty} e^{-i\beta_{in} z_0'} \\
 &\quad v(x_0, y_0, z_0 - z_0', r_0) H_0(z_0') dz_0' | \phi_n \rangle \langle \phi_n |] \quad (4.11)
 \end{aligned}$$

and $H_0(z_0')$ is the Heaviside function.

Therefore equation (4.9) is obtained as

$$T^0 = (2\pi)^{-3} \int db e^{i\frac{q \cdot b_0}{\hbar}} i v (e^{iX_0(b)} - 1) \quad (4.12)$$

If we substitute $\underline{k}_n = \underline{k}$ literally in \underline{g}^{-1} we shall obtain

$$\underline{g}_{AI}^{-1} = \underline{k} \cdot (\underline{k} - \underline{p}) - \underline{v} + i\eta \quad (4.13)$$

Further let us write

$$\underline{G}_o^{-1} = \underline{g}_{AI}^{-1} - N_c \quad (4.14)$$

$$\text{where } N_c = (\underline{p} - \underline{k}_f) \cdot (\underline{p} - \underline{k}_i) \quad (4.15)$$

Clearly corrections due to N_c are caused by momentum deviations from both initial and final directions.

Using (4.13) and (4.5) we can show that

$$\underline{g}^{-1} = \underline{g}_{AI}^{-1} + N_g^{-1} \quad (4.16)$$

$$\text{where } N = \lambda \underline{g}^{-1} + N_c \text{ and } \lambda = 1 - \cos \theta/2 ,$$

θ is the scattering angle of the projectile. We can thus write the expression for \underline{G}_o as $\underline{G}_o = \underline{g} + gNG_o$

This expression of \underline{G}_o can be substituted in equation (4.1). This will produce an expansion to the T matrix as a perturbation series

$$T = T^0 + T^1 + T^2 + T^3 + \dots \quad (4.18)$$

The first correction is obtained as

$$T' = - T^0 + J' \quad (4.19)$$

$$\text{where } J' = \langle \phi_f^{(-)} | V + N_c | \phi_i^+ \rangle \quad (4.20)$$

The general term in the expansion is

$$T^n = \sum_{m=2}^n \left(\frac{n-2}{m-2} \right) \lambda^{n-m} J^m \quad (4.21)$$

$$\text{where } J^m = \langle \psi_f^{(-)} | (\lambda V + N_c) [g(\lambda V + N_c)]^{m-1}$$

$$| \psi_i \rangle \quad (4.22)$$

From (4.3) we can write

$$\begin{aligned} J' &= (2\pi)^{-3} \langle \phi_f^{(-)} | \int e^{ik_f \cdot r_o} dv_o [1 - \frac{i}{k_n} \Sigma] | \phi_i^+ \rangle \\ &\quad \langle \phi_i^+ | \int_z^\infty e^{-i\beta_{in} z'} v(x_o, y_o, z_o') dz_o' e^{ik_i \cdot r_o} \\ &\quad [1 - \frac{i}{k_n} \Sigma] | \phi_i^+ \rangle \langle \phi_i^+ | \int_{-\infty}^z e^{-i\beta_{in} z_o'} \\ &\quad v(x_o, y_o, z_o') dz_o' e^{ik_i \cdot r_o} [1 + \frac{i}{k_n} \Sigma] | \\ &\quad \phi_i^+ \rangle \langle \phi_i^+ | \int_{-\infty}^\infty e^{-i\beta_{in} z_o'} dz_o' v(x_o, y_o, z_o') dz_o' \\ &\quad (\lambda V + N_c) e^{-ik_i \cdot r_o} [1 - \frac{i}{k_n} \Sigma] \int_{-\infty}^z e^{-i\beta_{in} z_o'} \\ &\quad v(x_o, y_o, z_o') dz_o' | \phi_i^+ \rangle \langle \phi_i^+ | \phi_i^+ \rangle \quad (4.23) \end{aligned}$$

The last terms in ϕ_f and ϕ_i are first order in V the change in action experienced by a particle which has travelled from $-\infty$ to z in case of X_+ and z to ∞ in case of X_- . We assume that the product of these are small in high energy approximation. Thus we have,

$$\begin{aligned} J^1 &= (2\pi)^{-3} \langle \phi_f | \int e^{iq \cdot b_0} e^{iX_0} e^{-ik_i \cdot r_0} \\ &\quad e^{-iX_+} (\lambda v + N_c) e^{ik_i \cdot r_0} e^{iX_+} dv \rangle \end{aligned} \quad (4.24)$$

Now we can show that

$$\begin{aligned} &e^{-i k_i \cdot r_0} e^{-i X_+} (\lambda v + N_c) e^{i k_i \cdot r_0} e^{i X_+} \\ &= Q \cdot [P_b + \nabla X_+(r)] - \nabla X_- \cdot P - t_1(r, r_j) \end{aligned} \quad (4.25)$$

where the operator $Q = [P + q + \nabla X_0(b)]$

$$\text{and } t_1(r, r_j) = -\lambda v + \nabla X_+ \cdot \nabla X_- \quad (4.26)$$

$$\text{Here } -i \nabla_j = -i \nabla_b - i \hat{k} \frac{\partial}{\partial z_j} \quad (4.27)$$

The operator Q plays a special role since it can be commuted leftward to produce a vanishing contribution to

the scattering amplitude. The details of the properties of Q are described by Wallace (1973). After the elimination of the term involving Q , equation (4.24) can be expressed as

$$\begin{aligned} J^1 &= (2\pi)^{-3} \langle \phi_f | \int e^{i\mathbf{q}\cdot\mathbf{b}_0} e^{iX_0} [\lambda v - \nabla X_+ \cdot \nabla X_-] \\ &= (2\pi)^{-3} \langle \phi_f | \int e^{i\mathbf{q}\cdot\mathbf{b}_0} e^{iX_0} t_1(\underline{x}, \underline{x}_j) | \phi_i \rangle \end{aligned} \quad (4.28)$$

Further we can simplify J^1 as

$$\begin{aligned} J^1 &= (2\pi)^{-3} \langle \phi_f | \int e^{i\mathbf{q}\cdot\mathbf{b}_0} \lambda v dv | \phi_i \rangle \\ &- i(2\pi)^{-3} \langle \phi_f | \sum \int e^{i\mathbf{q}\cdot\mathbf{b}_0} V \int_{-\infty}^{\infty} e^{-i\beta \sin z'_0} \\ &V(x_0, y_0, z'_0) | \phi_n \rangle \langle \phi_n | dz' | \phi_i \rangle \\ &+ (2\pi)^{-3} \frac{i}{k_n} \langle \phi_f | \sum \int e^{i\mathbf{q}\cdot\mathbf{b}_0} \\ &(\nabla X_+ \cdot \nabla X_-) \int_{-\infty}^{\infty} e^{-i\beta \sin z'_0} dz'_0 V(x_0, y_0, z'_0) \\ &dz'_0 | \phi_n \rangle \langle \phi_n | \phi_i \rangle \end{aligned} \quad (4.29)$$

The objects ∇X_+ and ∇X_- are classical momentum transfers for a particle which started at $z' = -\infty$ and travelled upto a position z and which started at the position z and then travelled upto a position $z' = \infty$ respectively. Using the same notations as those of Yates (1979) we can write T^0 and T' as

$$T^0 = T^{B1} + (T^{B2})_{HEA} \quad (4.30)$$

$$T' = [- \lambda T^0 + \lambda (T^{B2})_{HEA}] - (2\pi)^{-3} \langle \phi_f | \int$$

$$e^{ig \cdot b_0} (\nabla X_+ + \nabla X_-) dv_0 | \phi_n \rangle$$

$$| \phi_n \rangle | \phi_i \rangle \quad (4.31)$$

The terms of the order k_i^{-3} are neglected in the above equation. The last term in the above expression can be further simplified using the values of X_+ and X_i as

$$(2\pi)^{-3} \phi_f | \int e^{ig \cdot b_0} (\nabla X_+ + \nabla X_-) dv_0 | \phi_i \rangle$$

$$= \frac{(2\pi)^{-3}}{4k_n^2} [\langle \phi_f | \sum_n \int e^{ig \cdot b_0} db_0]$$

$$\begin{aligned}
 & \int_{-\infty}^{\infty} dz_o \left[\int_{-\infty}^z dz'_o \nabla V \cdot \int_{z_o}^{\infty} \nabla V dz'_o \right] \\
 & \phi_i > -i\beta_{in} \sum_n \int_{z_o}^{\infty} \nabla V dz'_o \cdot \int_{-\infty}^z \nabla (z'_o V) dz'_o \\
 & = -i\beta \int_{-\infty}^{z_o} \nabla V dz'_o \int_{-\infty}^{z_o} \nabla (z'_o V) dz'_o \\
 & = \text{Re } f_{W_2} - i\beta_{in} \text{Ref}_{W_2} \quad (4.32)
 \end{aligned}$$

where Ref_{W_2} is the real term of the Second Born term of Wallace.

The Second HHOB correction can be obtained by putting $m = 2$ in equation (4.22)

$$\begin{aligned}
 J^2 &= \langle \Psi_f | (\lambda V + N_c) g (\lambda V + N_c) | \psi_i \rangle \\
 &= -i \frac{(2\pi)^{-3}}{2 k_n} \langle \phi_f | \int e^{iq \cdot b_o} e^{iX_o} \\
 &\quad [Q_1 (p_1 + \nabla_1 X_+ (r_1) - \nabla_1 X_- (r_1) \cdot p_1 \\
 &\quad - t_1(r_1)) \int dz_2 \Theta(z_1 - z_2) [Q_2 \cdot (p_2 \\
 &\quad + \nabla_2 X_+ (r_2)) - \nabla_2 X_- (r_2) \cdot p_2 - t_1(r_2)]] | \phi_i \rangle
 \end{aligned}$$

$$\begin{aligned}
&= \frac{i}{2k_n} \langle \phi_f | \int db \left[\int_{-\infty}^{\infty} dz_1 (t_1(r) + \nabla_1 X_- \cdot P_1) \right. \\
&\quad \left. \int_{-\infty}^{z_1} t_1(r_2) dz_2 + \int_{-\infty}^{\infty} dz_1 (-\nabla_1 X_- \cdot \{ -[P, Q] \} \right. \\
&\quad \left. + [Q, P] \} - [t, Q] + Qt \left. \int_{-\infty}^z \nabla_2 X_+ dz_2 \right] \right] | \phi_i \rangle \\
&\quad (4.33)
\end{aligned}$$

The above equation can be further simplified using the same technique for J^1 term. Hence we will get

$$\begin{aligned}
J^2 &= -i \frac{(2\pi)^{-3}}{2 k_n} \langle \phi_f | \int db e^{iq \cdot r} \\
&\quad e^{i X_o(b)} \left[(-\lambda v + \nabla_+ X_+ \cdot \nabla_- X_-) \right]^2 / 2! \\
&\quad + \int t_2(r_1) dz_1 | \phi_i \rangle \quad (4.34)
\end{aligned}$$

Neglecting the terms of the order of k^{-3} and above that we can write the equation (4.34) as

$$\begin{aligned}
J^2 &= -i \frac{(2\pi)^{-3}}{4 k_n} \langle \phi_f | \int db e^{iq \cdot b} e^{i X_o(b)} \\
&\quad \left[\int_{-\infty}^{\infty} i dz_1 (-\lambda v + \nabla_+ X_+ \cdot \nabla_- X_-) \right]^2 | \phi_i \rangle
\end{aligned}$$

$$\begin{aligned}
 &= i \frac{(2\pi)^{-3}}{4k_n} \langle \phi_f | \int d\mathbf{b} e^{i\mathbf{q} \cdot \mathbf{b}} \\
 &\quad e^{ix_0(\mathbf{b})} [\int dz_1 i t_1(r_1)]^2 \\
 &\quad | \phi_i \rangle \tag{4.35}
 \end{aligned}$$

Simplifying the above equation further

$$\begin{aligned}
 \mathbf{j}^2 &= -i \frac{(2\pi)^{-3}}{4k_n} \langle \phi_f | [\int d\mathbf{b} e^{i\mathbf{q} \cdot \mathbf{b}} \\
 &\quad e^{ix_0(\mathbf{b})} \int_{-\infty}^{\infty} v^2 dz_1 + \int d\mathbf{b} \\
 &\quad e^{i\mathbf{q} \cdot \mathbf{b}} e^{ix_0(\mathbf{b})} \int_{-\infty}^{\infty} (\nabla x_+ \cdot \nabla x_-)^2 \\
 &\quad dz_1 - 2 \int d\mathbf{b} e^{i\mathbf{q} \cdot \mathbf{b}} e^{ix_0(\mathbf{b})} \\
 &\quad \int_{-\infty}^{\infty} dz_1 v (\nabla x_+ \cdot \nabla x_-)] \\
 &\tag{4.36}
 \end{aligned}$$

Substituting the value of $e^{ix_0(b)}$ in the above equation

$$\begin{aligned}
 J^2 &= -i \frac{(2\pi)^{-3}}{4k_n} \langle \phi_f | [\lambda^2 \int db e^{iq.b} \\
 &\quad \left\{ 1 - \frac{i}{k_n} \int_{-\infty}^{\infty} e^{-i\beta_{in} z'_0} V dz'_0 \right\} \int_{-\infty}^{\infty} V^2 dz \right. \\
 &\quad + \int db e^{iq.b} \left\{ 1 - \frac{i}{k_n} \int_{-\infty}^{\infty} e^{-i\beta_{in} z'_0} \right. \\
 &\quad \left. V dz'_0 \right\} \int_{-\infty}^{\infty} (\nabla X_+ \cdot \nabla X_-)^2 dz_1 - 2 \lambda \int db \\
 &\quad e^{iq.b} \left\{ 1 - \frac{i}{k_n} \int_{-\infty}^{\infty} e^{i\beta_{in} z'_0} V dz'_0 \right\} \\
 &\quad \left. \int_{-\infty}^{\infty} V (\nabla X_+ \cdot \nabla X_-) dz_1 \right] | \phi_i \rangle \quad (4.37)
 \end{aligned}$$

The third correction can be written in comparison with J^1 and J^2 as

$$\begin{aligned}
 J^3 &= -i (2\pi)^{-3} \langle \phi_f | \int db e^{iq.b} e^{ix_0(b)} \\
 &\quad [\int_{-\infty}^{\infty} dz_1 i t_1(r_1)]^3 / 3! | \phi_i \rangle \quad (4.38)
 \end{aligned}$$

In general we can write

$$J^\eta = - \frac{i(2\pi)}{2k_n} \frac{-3}{n!} \langle \phi_f | \int db e^{\frac{iq.b}{2}} e^{ix_o(b)} [\int dz_1 i t_1(x_1) + \dots + \dots] | \phi_i \rangle \quad (4.39)$$

The T matrix can be obtained by summing up all the J's.

Now the amplitude term can be obtained as

$$f = - (2\pi)^2 T = -(2\pi)^2 \sum_n T^n \quad (4.40)$$

If we include only J^0 and J' in T then the amplitude factor we will obtain as

$$f = f_{B1} + R_e l f_{HEA}^{(2)} (1 - \lambda) + I_m f_{HEA}^{(2)} (1 + \lambda) + R_e f_{w2} (1 - 2i \beta_{in}) \quad (4.41)$$

Inclusion of the J^2 will give the amplitude f as

$$f = f_{B1} + R_e l f_{HEA}^{(2)} (1 - \lambda) + I_m f_{HEA}^{(2)} (1 + \lambda) + R_e f_{w2} (1 - 2i \beta_{in}) - 2\pi^2 J^2 \quad (4.42)$$

Substituting the value of J^2 from (4.37) we will get

$$f = f_{B1} + R_e l f_{HEA}^{(2)} (1 - \lambda) + I_m f_{HEA}^{(2)} (1 + \lambda)$$

$$\begin{aligned}
& + R_e f_{w2} (1 - 2i\beta_{in}) - \frac{\lambda^2}{8k_n} f'_{B1} \\
& + i \frac{\lambda^2}{8\pi k_n^2} \int db e^{iq.b} \int_{-\infty}^{\infty} e^{-i\beta_{in} z_o'} V dz_o' \\
& \int V^2 dz = \frac{i}{8\pi k_n} \int db e^{iq.b} \int_{-\infty}^{\infty} e^{-i\beta_{in} z_o'} \\
& V dz_o' \int_{-\infty}^{\infty} (\nabla x_+ \cdot \nabla x_-)^2 dz_1 - \frac{i}{8\pi k_n} \int db e^{iq.b} \\
& \int_{-\infty}^{\infty} (\nabla x_+ \cdot \nabla x_-)^2 dz_1
\end{aligned}$$

Now consider the term

$$\begin{aligned}
& \frac{i}{8\pi k_n} \int db e^{iq.b} \int_{-\infty}^{\infty} (\nabla x_+ \cdot \nabla x_-)^2 dz \\
& = \frac{i}{8\pi k_n} \frac{1}{k_n^4} \int e^{iq.b} db \left\{ \nabla \int_{-\infty}^{z_o} e^{-i\beta_{in} z_o'} \right. \\
& \quad \left. V dz_o' \cdot \nabla \int_{z_o}^{\infty} e^{-i\beta_{in} z_o'} V dz_o' \right\}^2 \\
& = \frac{i}{8\pi k_n} \int db e^{iq.b} \left\{ \nabla \int_{-\infty}^{z_o} (1 - i\beta_{in} z_o') V dz_o' \nabla \right. \\
& \quad \left. \int_{z_o}^{\infty} (1 - i\beta_{in} z_o') V dz_o' \right\}^2
\end{aligned}$$

$$\begin{aligned}
&= \frac{i}{8\pi k_n^5} \int db e^{iq.b} \left[\int_{-\infty}^{z_0} \nabla V dz'_0 + \int_{z'_0}^{\infty} \nabla V dz'_0 \right] \\
&\quad - i \nabla \beta_{in} \int_{-\infty}^{z_0} z'_0 V dz'_0 + \nabla \int_{z'_0}^{\infty} V dz'_0 - i \beta_{in} \\
&\quad \int_{-\infty}^{z_0} \nabla z'_0 V dz'_0 - \nabla \int V dz'_0 \\
&= (R_e f_{w3} - i 4 \beta_{in} R_e f_{w3}) \tag{4.46}
\end{aligned}$$

Substituting the value in (4.45) we will get the amplitude as

$$\begin{aligned}
f &= f_{B1} + R_e l f_{HEA}^{(2)} (1 - \lambda) + I_m f_{HEA}^{(2)} (1 + \lambda) \\
&\quad + R_e f_{w2} (1 - 2i\beta_{in}) - f_{w3} + 4i\beta_{in} f_{w3} \\
&\quad + \frac{i}{8\pi k_n^2} \int db e^{iq.b} \left[\int_{-\infty}^{\infty} e^{-i\beta_{in} z'_0} V dz'_0 + \int_{-\infty}^{\infty} V^2 dz' \right] \\
&\quad - \frac{1}{8\pi k_n^2} \int db e^{iq.b} \left[\int e^{i\beta_{in} z'_0} V dz'_0 + \int_{-\infty}^{\infty} \right. \\
&\quad \left. (\nabla X_+ \cdot \nabla X_-)^2 dz_1 - \frac{\lambda^2}{8\pi k_n^2} f_{B1}' \right] \tag{4.47}
\end{aligned}$$

In the above equation all the terms of the order of k_n^{-2}
are dropped out. This is not too much justified

because if one takes higher order terms in J^3 there
are going to be terms of the order of k_n^{-2} .

However to maintain the symmetry we somehow justify
the assumption. Hence

$$\begin{aligned} f &= f_{B1} + R_e \underset{\text{HEA}}{I} f^{(2)} (1 - \lambda) + I_m \underset{\text{HEA}}{f}^{(2)} (1 + \lambda) \\ &\quad + R_e f_{w2} (1 - 2i\beta_{in}) - R_e f_{w3} + 4i\beta_{in} \\ &\quad R_e f_{w3} - \frac{\lambda^2}{8\pi k_n} f'_{B1} \end{aligned} \quad (4.48)$$

The difference between f_2 and f' is that the latter contains the V term as the interaction term and further it is of the order of $\frac{1}{k_n}$. In comparison

with f_{B1} this term contribution is small and thus we will get

$$\begin{aligned} f &= f_{B1} + R_e \underset{\text{HEA}}{I} f^{(2)} (1 - \lambda) + I_m \underset{\text{HEA}}{f}^{(2)} (1 + \lambda) \\ &\quad + R_e f_{w2} (1 - 2i\beta_{in}) - R_e f_{w3} (1 - 4i\beta_{in}) \end{aligned} \quad (4.49)$$

Similarly if we will take J^3 contribution we will obtain the amplitude f as

$$f = f_{B1} + R_e \underset{\text{HEA}}{I} f^{(2)} (1 - \lambda) + I_m \underset{\text{HEA}}{f}^{(2)} (1 + \lambda)$$

$$\begin{aligned}
 & + R_e f_{w2} (1 - 2i\beta_{in}) - R_e f_{w3} (1 - 4i\beta_{in}) \\
 & + R_e f_{w4} (1 - 8i\beta_{in}) \tag{4.50}
 \end{aligned}$$

We can see from the above expression that the various amplitudes are corresponding to the orders of K^0 , K^{-1} , K^{-2} , \bar{K}^3 etc in $X_0(b)$. We remark that f is explicitly a function of λ . Hence for small momentum transfer, $\lambda = 0$. And thus we have the T matrix as

$$T = \sum_n J_n(b, 0) = -i e^{ix_0(b)} [e^{it_1(b)}] \tag{4.51}$$

Hence the amplitude will be

$$\begin{aligned}
 f = f_{B1} & + R_e f_{HEA}^{(2)} + I_m f_{HEA}^{(2)} + R_e f_{w2} (1 - 2i\beta_{in}) \\
 & - R_e f_{w3} (1 - 4i\beta_{in}) R_e f_{w4} (1 - 8i\beta_{in}) \tag{4.52}
 \end{aligned}$$

Obviously we can verify that when $\beta_i \rightarrow 0$ it exactly turns out to be the eikonal approximation.

The principle difference between HHOB and the present form lies in the handling of momentum transfer dependence.

If we want to consider the large momentum transfer we should consider λ also. Now we will follow

the same argument as the Wallace. The class of terms that would survive can be given by $\sum_n J^n(b, o)$ plus the additional undetermined functions which however will be of the order of K_n^{-4} or small. Thus the corrected HHOB amplitude can be conjectured to the successive approximation upto the order of K_n^{-3} .

The important high lights of the present method is that the corrections are done to the HHOB approximation in analogous with the eikonal approximation.

4.3 Calculations

Hydrogen Atom :

The ground state wave function for hydrogen atom can be written as

$$\phi^H(x_1) = \frac{1}{\sqrt{\pi}} \exp(-r) \quad (4.53)$$

The interaction potential can be written as

$$V = -\frac{1}{r_o} + \frac{1}{|r_o - r_1|} \quad (4.54)$$

The first Born amplitude will be obtained as

$$f_{B1} = \frac{2(q^2 + 8)}{(q^2 + 4)}$$

The expressions for $R_e^{(2)}$ and $I_m^{(2)}$ are given in equation (3.21) and (3.19) respectively. The expression for $R_e f_{w2}$ is

$$R_e^H f_{w2} = k_i^2 \int_0^\infty J_0(q\underline{b}) A(\underline{b}) \underline{b} d\underline{b} \quad (4.56)$$

where

$$\begin{aligned} A(\underline{b}) &= \int_{1s} |\phi_{1s}(r_1)|^2 x_1(b, r_1) dr_1 \\ &= \pi^{-1} \int db_1 b_1 \int_{-\infty}^\infty dz_1 \exp[-2(b_1^2 + z_1^2)] \\ &\quad \int dw X_1(b, r_1) \end{aligned} \quad (4.57)$$

Here w is the angle between \underline{b} and \underline{b}_1 and

$$x_1(b, r_1) = \frac{\pi}{(b\beta)^{1/2}} [P_{-1/2}(u) - \hat{\underline{b}} \cdot \hat{\underline{\beta}} P_{1/2}(u)] \quad (4.58)$$

$$\text{where } u = (b^2 + \beta^2 + z_1^2) / 2b\beta$$

Since $\hat{\underline{\beta}} = \underline{b} - \underline{b}_1$ we have

$$\hat{\underline{b}} \cdot \hat{\underline{\beta}} = (b^2 - b\underline{b}_1 \cos w) / b\beta = d\beta/d\underline{b} \quad (4.59)$$

The detailed calculations are given by Byron et al (1983)

The final expression is

$$\operatorname{Re}^H f_{W2} = \frac{2}{k_i^2(q^2 + 4)} + \frac{16}{k_i^2(q^2 + 4)^2} \quad (4.60)$$

Finally for the consistent picture of DCS $O(k_i^2)$ we have included the exchange amplitude (Byron and Joachain 1977) and third Glauber eikonal series term (Yates 1974). The corresponding expressions are

$$g_{och} = -\frac{32}{k_i^2} (q^2 + 4)^{-2} \quad (4.61)$$

and

$$f_{GES}^{(3)} = \frac{ik_i}{2\pi} \int db_o \exp(iq \cdot b_o) \frac{(ix)^3}{3!} \quad (4.62)$$

$$\text{where } X = -\frac{1}{k_i} \int_{-\infty}^{\infty} V dz_o \quad (4.63)$$

Thus using the equations (4.1) to (4.63) we have obtained the DCS and TCS in Wallace corrected HHOB term for the elastic of electrons by hydrogen atom at 100 eV to 400 eV and 100 eV to 1000 eV respectively.

Helium Atom :

The well known Hartree - Fock wave function for the ground state of helium atom can be written as

$$\phi_{1s}^{\text{He}}(\underline{r}_1, \underline{r}_2) = \frac{(P+Q)(R+S)}{4\pi} \quad (4.64)$$

The values of P, Q, R and S are given in equation (3.14)

The interaction between the incident electron and target atom can be written as

$$V = -\frac{2}{r_0} + \frac{1}{|\underline{r}_0 - \underline{r}_1|} + \frac{1}{|\underline{r}_0 - \underline{r}_2|} \quad (4.65)$$

where r_0, r_1, r_2 had the usual meaning.

The expressions for $f_{B1}^{(2)}$, $R_{\text{elf}}^{\text{HEA}}$, $I_m f_{\text{HEA}}^{(2)}$ are given in equations (3.17), (3.28) and (3.24) respectively.

$\text{Re } f_{W2}^{\text{He}}$ can be obtained by evaluating the expression

$$\text{Re } f_{W2}^{\text{He}} = k_i^{-2} \int_0^\infty J_0(q b) A(b) b \, db \quad (4.66)$$

$$\text{where } A(b) = \int |\phi_{1s}(\underline{r}_1, \underline{r}_2)|^2 x_1(b, \underline{r}_1, \underline{r}_2) \, d\underline{r}_1 \, d\underline{r}_2 \quad (4.67)$$

$$\text{and } x_1(b, \underline{r}_1, \underline{r}_2) = \frac{1}{2} \int_{-\infty}^{\infty} (\nabla_x^+ \cdot (\nabla_x^-)) \, dz \quad (4.68)$$

Following the same method used for the calculation of

$\text{Re}^H f_{W2}$ we can obtain the final expression for $\text{Re}^{\text{He}} f_{W2}$

as follows.

$$\begin{aligned} \text{Re}^{\text{He}} f_{W2} &= \text{Re}^1 f_{W2} + \text{Re}^2 f_{W2} + \text{Re}^3 f_{W2} + \text{Re}^4 f_{W2} \\ &\quad + \text{Re}^5 f_{W2} + \text{Re}^6 f_{W2} \end{aligned} \quad (4.69)$$

Here

$$\text{Re}^1 f_{W2} = \frac{16 A^4}{k_i^2 \alpha^6 (q^2 + \alpha^2)} + \frac{32 A^4}{k_i^2 \alpha^4 (q^2 + \alpha^2)^2}$$

$$\text{Re}^2 f_{W2} = \frac{16 B^4}{k_i^2 \beta^6 (q^2 + \beta^2)} + \frac{32 B^4}{k_i^2 \beta^4 (q^2 + \beta^2)^2}$$

$$\text{Re}^3 f_{W2} = \frac{64 A^2 B^2}{k_i^2 \beta^6 (q^2 + \beta^2)} + \frac{128 A^2 B^2}{k_i^2 \beta^4 (q^2 + \beta^2)^2}$$

$$\begin{aligned} \text{Re}^4 f_{W2} &= \frac{16 A^2 B^2}{k_i^2} \left[\frac{1}{\alpha^6 (q^2 + \alpha^2)} + \frac{2}{\alpha^4 (q^2 + \alpha^2)^2} \right. \\ &\quad \left. + \frac{1}{\gamma^6 (q^2 + \gamma^2)} + \frac{2}{\gamma^4 (q^2 + \gamma^2)^2} \right] \end{aligned}$$

$$\begin{aligned}
 \text{Re}^5 f_{W2} &= \frac{32 A^3 B}{k_i^2 \alpha^6} \left[\frac{1}{(q^2 + \alpha^2)} + \frac{2 \alpha^2}{(q^2 + \alpha^2)^2} \right] \\
 &\quad + \frac{32 A B^3}{\beta^6 k_i^2} \left[\frac{1}{q^2 + \beta^2} + \frac{2 \beta^2}{(q^2 + \beta^2)^2} \right] \\
 \text{Re}^6 f_{W2} &= \frac{32 A^3 B}{k_i^2 \alpha^6} \left[\frac{1}{(q^2 + \alpha^2)} + \frac{2 \alpha^2}{(q^2 + \alpha^2)^2} \right] \\
 &\quad + \frac{32 B^3 A}{k_i^2 \beta^6} \left[\frac{1}{q^2 + \beta^2} + \frac{2 \beta^2}{(q^2 + \beta^2)^2} \right]
 \end{aligned}$$

The constants A and B are given in equation (3.14).
 Here $\alpha = yy'$, $\beta = yy'''$, $\gamma = yy''$ where $y = 2$;
 $y' = 1.41$; $y'' = 2.61$; $y''' = y' + y''/2$

For the calculation of DCS we have included third glauber term and the exchange term. The expressions are given in equation (3.31) and (3.34) respectively. The DCS is calculated for 200 eV and 400 eV.

Li atom :

The ground state wave function for Li atom is taken as that of Veselov et al (1961)

$$\phi = \frac{1}{\sqrt{3!}} \det (\psi_{1s\uparrow}, \psi_{1s\downarrow}, \psi_{2s\uparrow})$$

with

$$\psi_{1s} = \left(\frac{\alpha^3}{\pi} \right)^{1/2} e^{-\alpha r}$$

$$\psi_{2s} = \left[\frac{3\beta^5}{\pi(\alpha^2 - \alpha\beta + \beta^2)} \right]^{1/2} (1-\alpha + \frac{\beta}{3}) r e^{-\beta r}$$

where $\alpha = 2.694$ and $\beta = 0.767$

The interaction potential is taken as

$$V = \frac{-3}{r_0} + \frac{1}{|r_0 - r_1|} + \frac{1}{|r_0 - r_2|} + \frac{1}{|r_0 - r_3|}$$

The rotations have the usual meanings. The expressions
 $f_{B1}^{(2)}$, $Re f_{HEA}^{(2)}$, $I_m f_{HEA}^{(2)}$ are given in equations

(2.11), (2.19) and (2.15) respectively. The third

Glauber term is given in equation (2.21).

$$Re \frac{Li}{W2} f_{W2} = k_i^{-2} \int J_0(q \underline{b}) A(\underline{b}) \underline{b} d\underline{b}$$

$$\text{where } A(\underline{b}) = \iiint x_1(\underline{b}, \underline{r}_1, \underline{r}_2, \underline{r}_3) \phi^* \phi dv$$

$$= A^1(\underline{b}) + A^2(\underline{b}) + A^3(\underline{b})$$

where

$$A^1(b) = \frac{\alpha^3}{\pi} \int b_1 db_1 dz_1 e^{-\lambda_1 r_1} x_1(b, r_1)$$

$$A^2(b) = \frac{\alpha^3}{\pi} \int x_1(b, r_2) e^{-\lambda_2 r_2} b_1 db_1 dz_1$$

$$A^3(b) = \frac{N^2}{\pi} DOP(\lambda_3, \lambda_2) \int x_1(b, r_3) e^{-\lambda_3 r_3} dv$$

where $\lambda_1 = 2\alpha$; $\lambda_2 = 2\beta$; $\lambda_3 = \alpha + \beta$

Here the cross term calculations are neglected since they are less significant. Proceeding the same way as that of $Re_{W2}^H f$ we can find out $Re_{W2}^{Li} f$.

The final expression for $Re_{W2}^{Li} f$ is obtained as

$$Re_{W2}^{Li} f = \int b db J_0(qb) A(b)$$

$$= \frac{2}{\lambda_1^3} \left[\frac{1}{q^2 + \lambda_1^2} + \frac{2\lambda_1^2}{(q^2 + \lambda_1^2)^2} \right]$$

$$+ 64 N^2 DOP(\lambda_3, \lambda_2) \frac{1}{\lambda_2^6} \left[\frac{1}{q^2 + \lambda_2^2} + \right.$$

$$\left. \frac{2\lambda_2^2}{(q^2 + \lambda_2^2)^2} \right]$$

The DCS is calculated for elastic scattering by Li atom from 100 eV to 400 eV.

4.4 Results and Discussions :

Hydrogen Atom :

The present results for the DCS for the elastic scattering of electrons by hydrogen atoms at 100 eV, 200 eV and 400 eV are given in table (4.1), (4.2) and (4.3) along with other available theoretical and experimental data. In table (4.4) we have shown the present results for the TCS in the energy range 100 eV to 700 eV. The present results for the elastic scattering of $\bar{e} - H$ are also shown in figures (4.1) to (4.3). The values are shown at small angles because (i) HHOB is good for only small angles and (ii) the correctness of the Wallace correction has not been established for large angles.

In table (4.5) we have exhibited the individual amplitudes. $Re lf_{HEA}^{(2)}$ term is of the order of k_i^{-1} only and $Re f_{W2}^{(2)}$ is of the order of k_i^{-2} . If β_i is set equal to zero the $Re lf_{HEA}^{(2)}$ will vanish and the leading term of the real part of second Born term is then proportional to k_i^{-2} . The imaginary part of $f_{HEA}^{(2)}$ is of the order of k_i^{-1} . If we set $\beta_i = 0$ this term exactly

becomes Glauber's estimate of the second Born term.

It can be seen from the tables and figures that the present results agree very well with the experimental data. It may be noted that the present calculations yield better results than the simple HHOB approximation (Rao and Desai 1983). The main difference between the present approximation and simple HHOB approximation is that $\frac{1}{k_i^2}$ real term of HHOB is replaced by $\frac{1}{k^2}$ real term of Wallace term.

From table (4.5) we can see that the $\frac{1}{k_i^2}$ term of HHOB is smaller than $R_e f_{w2}$. Hence HHOB overestimate at higher angles and underestimate at smaller angles than the present results. The R_e and I_m are different from those of HHOB terms by $(1 + \lambda)$ and $(1 - \lambda)$ respectively.

Looking at figures (4.1) to (4.3) we see that our results agree very well with experimental data upto angle 50° whereas the UEBS (Byron et al 1982) agrees up certain angles. For 100 eV the difference between our results and experimental values of Williams is less than 1 %. For 200 eV also the difference between our results and Williams is very less. The

HHOB results underestimates in this region. We can see that UEBS results are lower in the whole angular region. For 400 eV we can see that the DCS values of all workers agree very well.

Helium atom :

The DCS for the elastic \bar{e} - He atom at 200 eV and 400 eV are calculated using the present results are shown in Tables(4.6) and (4.7) and Figures (4.4) and (4.5) along with other theoretical and experimental data. Here also we have shown the results for small angles.

From Tables and Figures we can see that our results fairly compare with the experimental values. For 200 eV our results are slightly higher than that of Jansen et al (1976) and lower than that of Crooks et al (1972). But for 400 eV our results are lower than that of Jansen et al. For 200 eV the EBS results are almost same as that of our results. For 400 eV EBS results are less than that of present results. From 40° onwards the experimental values and theoretical values have significant difference.

In Table (4.8) we have shown the individual amplitude. We can see that Ref_{w2} are lower than that

(2) of $R_{e2} f_{HEA}$ for the whole energy range for 200 eV and 400 eV. Hence the effect of $R_e f_{w2}$ is to reduce the differential cross sections. The difference between $R_e f_{w2}$ and $R_{e2} f_{HEA}^{(2)}$ is significant from angles larger than 40° . The present real and imaginary terms differ from HHOB terms by $(1 - \lambda)$ and $(1 + \lambda)$ respectively. Hence the present DCS results are slightly more than HHOB results at small angles and smaller than HHOB results at large angles. Hence we can justify the inclusion of trajectory correction for the calculation of DCS for the elastic scattering of electrons by helium atoms. We have shown the results for angles up to 50° since the trajectory correction is established for small angles only.

Li Atom :

In Tables (4.9) to (4.12) we have given the DCS for the elastic scattering of electrons by lithium atom along with other results. The results are also shown in Figures (4.6) to (4.9). Here also we have given the results up to 90° . The reasons are same as those of hydrogen atom. For 100 eV we can see that the present results are slightly lower than that of HHOB at 5° and higher than that of HHOB afterwards up to 60° . The difference between the present

and HHOB is nearly 5 to 15 %. The EBS results are higher than ours from 40° onwards.

For 200 eV also our present results increases HHOB up to 60° and decreases afterwards. For 300 eV and 400 eV our results are greater than HHOB from 20° onwards.

In Tables (4.13a, b, c and d) we have shown the individual amplitude terms. We can see that $R_{e_2 f}^f$ and $R_{e_2 f}^{HEA}$ are having significant difference at large angles. Hence we can conclude that the trajectory correction included for the calculation of DCS gives better results than the ordinary HHOB calculation.

Table : 4.1 : Differential cross sections ($a_0^2 s_r^{-1}$) for elastic $\bar{e} - H$
scattering E = 100 eV.

Angle (deg)	Present	HHOB	UEBS	Williams
5	3.2518	4.3553	4.46	-
10	1.9981	2.4399	2.40	-
20	8.7995(-1)	9.6622(-1)	8.46(-1)	1.10
30	4.1863(-1)	4.4954(-1)	3.50(-1)	5.09(-1)
40	1.8051(-1)	2.3612(-1)	1.63(-1)	2.88(-1)
50	9.8377(-2)	1.3814(-1)	8.43(-2)	1.32(-1)
60	5.8383(-2)	8.9610(-2)	4.80(-2)	7.22(-2)
80	2.6311(-2)	4.7520(-2)	1.96(-2)	2.95(-2)

Table : 4.2 : DCS ($a_0^2 s_r^{-1}$) for elastic $\bar{e} - H$ E = 200 eV

Angle (deg)	Present	HHOB	UEBS	Williams
5	1.8829	2.1286	2.19	-
10	1.0814	1.1377	1.12	-
20	4.1379(-1)	4.1731(-1)	3.80(-1)	4.19(-1)
30	1.6071(-1)	1.7089(-1)	1.43(-1)	1.72(-1)
40	7.3286(-2)	8.0150(-2)	6.10(-2)	7.06(-2)
50	3.3554(-2)	4.3950(-2)	2.95(-2)	3.14(-2)
60	1.8505(-2)	2.7250(-2)	1.59(-2)	1.87(-2)
80	7.7731(-3)	1.3610(-2)	6.04(-3)	1.25(-2)

Table : 4.3 : DCS ($a_0^2 s_r^{-1}$) for elastic $\bar{e} - H$ scattering,
 $E = 400$ eV.

Angle (deg)	Present	HHOB	UEBS	Williams
5	1.1666	1.1973	1.21	-
10	6.3939	6.3920(-1)	6.27(-1)	-
20	1.7412(-1)	1.7878(-1)	1.67(-1)	1.96(-1)
30	5.2436(-2)	5.8350(-1)	5.03(-2)	6.17(-2)
40	1.9313(-2)	2.4491(-1)	1.88(-2)	2.06(-2)
50	9.0573(-2)	1.2602(-1)	8.45(-3)	9.47(-3)
60	4.8589(-3)	7.5421(-2)	4.39(-3)	4.38(-3)
80	1.9568(-3)	3.6210(-2)	1.62(-3)	1.57(-3)

Table : 4.4 : Total cross section for elastic $\bar{e} - H$ scattering (in a_0^{-2}).

Energy	Present	HHOB	UEBS (1977)	de Heer et al. (1977)
100	7.2372	7.5615	7.19	6.85
200	4.2875	4.3685	4.27	4.18
300	3.1063	3.1423	3.10	3.06
400	2.4590	2.4793	2.45	2.43
500	2.0465	2.0595	-	-
600	1.1759	1.7681	-	-
700	1.5464	1.5531	-	-

Table : 4.5 : The behaviour of the scattering amplitudes for \bar{e} - H scattering at 100 eV.

Θ	f_{B1}	$R_{el} f_{HEA}^{(2)}$	$R_e f_{W2}$	$R_{e2} f_{HEA}^{(2)}$	$I_m f_{HEA}^{(2)}$	$f_{GES}^{(-ve)}$	f_{exch}
5	.9794	.4156	.1994	.1959	1.3464	.0237	4.3553
10	.9220	.1398	.1863	.1810	.9331	.0634	2.4399
20	.7442	.0182	.1468	.1405	.4642	.1178	0.9662
30	.5594	.0085	.1258	.1091	.2831	.1283	0.4495
40	.4132	.0108	.0758	.0935	.2092	.1176	0.2361
50	.3095	.0121	.0548	.0880	.1772	.1053	0.1381
60	.2382	.0119	.0408	.0873	.1488	.0938	0.0896
80	.1545	.0099	.0252	.0897	.1181	.0768	0.0475

Table : 4.5 : Contd... .

E = 200 eV.

Θ	f_{B1}	$R_{el} f_{HEA}^{(2)}$	$R_e f_{W2}^{(2)}$	$R_e f_{HEA}^{(2)}$	$I_m f_{HEA}^{(2)}$	$f_{GES}(-ve)$	f_{exch}
5	.9595	.1141	.0893	.0956	.8410	.0200	.1287
10	.8543	.0163	.0856	.0818	.4737	.0459	.1100
20	.5863	.0018	.0562	.0531	.2090	.0643	.0653
30	.3787	.0049	.0344	.0448	.1378	.0560	.0345
40	.2513	.0053	.0217	.0433	.1084	.0481	.0184
50	.1759	.0048	.0145	.0444	.0898	.0408	.0103
60	.1298	.0039	.0104	.0456	.0761	.0355	.0062
80	.0806	.0024	.0062	.0474	.0574	.0283	.0027

Table : 4.5 : Contd...•

 $E = 400 \text{ eV}$

Θ	1	2	3	4	5	6	7
5	.9219	.0161	.0466	.0451	.4557	.0159	.0609
10	.7427	.0011	.0366	.0342	.2212	.0293	.0454
20	.4054	.0027	.0186	.0225	.1002	.0295	.0191
30	.2249	.0029	.0082	.0217	.0748	.0227	.0077
40	.1375	.0023	.0039	.0227	.0591	.0182	.0035
50	.0927	.0018	.0036	.0235	.0484	.0152	.0017
60	.0670	.0014	.0025	.0241	.0409	.0129	.0009
80	.0409	.0009	.0013	.0246	.0319	.0101	.0004

Table : 4.6 : DCS ($a_0^2 s_r^{-1}$) for the elastic $\bar{e} - He$ scattering
 $E = 200$ eV.

Angle (deg)	Present HHOB	EBS	Crooks and Rudd(1972)	Janssen et al (1976)
10	1.3249	1.3113	1.34	1.93
20	6.1141(-1)	6.0937(-1)	5.83(-1)	7.18(-1)
30	3.1662(-1)	3.1266(-1)	2.88(-1)	3.25(-1)
40	1.7582(-1)	1.8634(-1)	1.54(-1)	-
50	1.0400(-1)	1.0794(-1)	8.81(-2)	1.08(-1)
				8.85(-2)

Table : 4.7 : DCS ($a_0^2 s_r^{-1}$) for the elastic $\bar{e} - \text{He}$ scattering
 $E = 400$ eV.

Angle (deg)	Present	HNOB	EBS (1974)	Bromberg (1974)	Janssen et al (1976)
10	6.8589(-1)	6.7601(-1)	7.61(-1)	8.10(-1)	7.87(-1)
20	2.8982(-1)	2.8990(-1)	3.79(-1)	3.67(-1)	3.65(-1)
30	1.2847(-1)	1.3190(-1)	1.78(-1)	1.76(-1)	2.47(-1)
40	6.1727(-2)	6.6050(-2)	8.79(-2)	8.85(-2)	1.69(-1)
50	3.5025(-2)	3.7670(-2)	4.76(-2)	4.81(-2)	9.85(-2)

Table : 4.8 : The behaviour of the scattering amplitudes for $\alpha - \text{He}$ scattering
at E = 200 eV

α	f_{B1}	$R_{el} f_{HEA}^{(2)}$	$R_e f_{W2}$	$R_{e2} f_{HEA}^{(2)}$	$I_m f_{HEA}^{(2)}$	$f_{GES}(-ve)$	f_{exch}
10	.7373	.13538	.0782	.0835	.6598	.0993	.1248
20	.6103	.0364	.0217	.0513	.4067	.0983	.0991
30	.4743	.0210	.0097	.0488	.2915	.0965	.0725
40	.3622	.0183	.0055	.0503	.2413	.0943	.0513
50	.2793	.0167	.0036	.0528	.2138	.0923	.0363

Table : 4.8 : Contd....

at E = 400 eV.							
10	.6893	.0273	.0181	.0299	.3692	.0495	.0575
20	.4944	.0093	.0027	.0243	.2091	.0484	.0382
30	.3350	.0093	.0019	.0281	.1574	.0468	.0231
40	.2310	.0086	.0007	.0271	.1361	.0448	.0139
50	.1660	.0075	.0005	.0287	.1273	.0424	.0087

Table : 4.9 : DCS ($a_0^2 s_r^{-1}$) for the elastic $\bar{e} - \text{Li}$ scattering $E = 100 \text{ eV}$.

q	Present	HHOB	MGA (IC)	MGA (SPSM)	EBS
5	53.4605	53.7789	4.49(1)	5.53(1)	5.29(1)
10	25.2455	22.7605	1.75(1)	2.22(1)	1.82(1)
20	5.2461	4.4368	3.48	5.30	3.73
30	1.8858	1.7316	8.74(-1)	1.70	1.85
40	7.6135(-1)	7.0600(-1)	3.02(-1)	7.20(-1)	-
50	5.5878(-1)	5.2971(-1)	1.31(-1)	3.66(-1)	-
60	4.8986(-1)	4.1575(-1)	6.66(-2)	2.12(-1)	8.89(-1)
70	2.8163(-1)	2.6970(-1)	3.80(-2)	1.35(-1)	-
80	1.3575(-1)	1.4017(-1)	2.88(-2)	9.30(-2)	-
90	6.9686(-2)	6.2943(-2)	1.61(-2)	6.78(-2)	6.16(-1)

Table : 4.10 : DCS ($a_0^2 s_r^{-1}$) for the elastic e - Li scattering E = 200 eV.

θ	Present	HOB	MGA (IC)	MIA (SPSM)	EBS
5	33.5780	33.9254	2.60(1)	3.12(1)	2.86(1)
10	14.0121	13.4760	9.47	1.20(1)	9.93
20	2.5895	2.5331	1.20	2.04	1.36
30	9.6611(-1)	9.4446(-1)	2.51(-1)	5.95(-1)	6.70(-1)
40	4.0414(-1)	4.3140(-1)	8.18(-1)	2.54(-1)	3.90(-1)
50	2.4267(-1)	2.7583(-1)	3.49(-1)	1.33(-1)	2.70(-1)
60	1.3339(-1)	1.0005(-1)	1.77(-2)	7.95(-2)	2.06(-1)
70	7.3368(-2)	9.7476(-2)	1.02(-2)	5.15(-2)	1.68(-1)
80	3.4389(-2)	5.4286(-2)	6.42(-3)	3.56(-2)	1.42(-1)
90	2.0062(-2)	3.5689(-2)	4.37(-3)	2.58(-2)	1.24(-1)

Table : 4.11 : DCS ($a_0^2 s_F^{-1}$) for the elastic
 $\bar{e} - Li$ scattering E = 300 eV.

Table : 4.12 : DCS ($a_0^2 s_F^{-1}$) for
the elastic $\bar{e} - Li$
scattering E = 400 eV.

θ	Present	HHOB	θ	Present	HHOB
5	26.8343	26.9836	5	22.8526	22.8526
10	9.3749	9.6721	10	6.6259	6.6259
20	1.6257	1.5465	20	1.0636	1.0618
30	5.7655(-1)	5.6810(-1)	30	4.3460(-1)	4.3828(-1)
40	2.6227(-1)	2.5889(-1)	40	3.1567(-1)	3.1653(-1)
50	1.5184(-1)	1.5005(-1)	50	1.1674(-1)	1.1624(-1)
60	8.0489(-2)	7.9416(-2)	60	5.3556(-2)	5.3131(-2)
70	4.1052(-2)	4.0394(-2)	70	2.9839(-2)	2.9754(-2)
80	2.9663(-2)	2.9217(-2)			
90	1.5741(-2)	1.5438(-2)			

Table : 4.13 : a - The behaviour of the scattering amplitudes for \bar{e} - Li scattering
at 100 eV.

e	f_{B1}	$R_{e1} f_{HEA}^{(2)}$	$R_e f_{w2}$	$R_{e2} f_{HEA}^{(2)}$	$I_m f_{HEA}^{(2)}$	f_{G3}
5	5.3104	1.3156	3.7431(-1)	4.0410(-1)	4.6180	1.47
10	4.3589	1.3048	3.01415(-1)	2.2464(-1)	2.0532	1.79
20	2.3875	1.0472	1.7963(-1)	1.0167(-1)	1.0213	1.77
30	1.3077	8.8979(-1)	9.6641(-2)	9.7697(-2)	8.9757(-1)	1.53
40	8.2825(-1)	7.9024(-1)	5.6112(-2)	2.2799(-2)	7.6369(-1)	1.40
50	5.9833(-1)	7.0569(-1)	3.6030(-2)	1.1174(-2)	6.8776(-1)	1.33
60	4.6904(-1)	6.2912(-1)	2.5201(-2)	6.1381(-3)	5.4058(-1)	1.16
70	3.8601(-1)	5.6079(-1)	1.8831(-2)	3.3762(-3)	4.6890(-1)	1.11
80	3.2863(-1)	5.0147(-1)	1.4809(-2)	1.9556(-3)	4.1579(-1)	1.00
90	2.8809(-1)	4.5113(-1)	1.2126(-2)	1.1822(-3)	3.7579(-1)	9.55(-1)

Table : 4.13 : b - The behaviour of the scattering amplitudes for \bar{e} - Li scattering at 200 eV.

Q	f_{B1}	$R_{el} f_{HEA}$	(2)	$R_{e2f} f_{HEA}$	$I_m f_{HEA}$	(2)	$I_m f_{HEA}$	(2)	f_{G3}
5	4.9598	9.7728(-1)	1.7619(-1)	2.1095(-1)	2.1655	8.17(-1)			
10	3.4641	8.4804(-1)	1.2725(-1)	5.9404(-2)	8.8262(-1)	9.30(-1)			
20	1.4213	6.4876(-1)	5.3079(-2)	2.3394(-2)	6.3401(-1)	7.81(-1)			
30	7.4431(-1)	5.4471(-1)	2.4382(-2)	1.1100(-2)	5.0629(-1)	6.64(-1)			
40	4.9194(-1)	4.5856(-1)	1.3521(-2)	3.9001(-3)	3.9209(-1)	6.44(-1)			
50	3.6469(-1)	3.8315(-1)	8.6311(-3)	1.5540(-3)	3.1542(-1)	5.34(-1)			
60	2.8809(-1)	3.2009(-1)	6.0630(-3)	6.6010(-4)	2.6422(-1)	4.85(-1)			
70	2.3452(-1)	2.6932(-1)	4.5565(-3)	2.8025(-4)	2.2849(-1)	4.45(-1)			
80	1.9748(-1)	2.2935(-1)	3.6010(-3)	1.2321(-4)	2.0245(-1)	4.25(-1)			
90	1.7029(-1)	1.9818(-1)	2.9001(-3)	6.1730(-4)	1.8280(-1)	3.92(-1)			

Table : 4.13 : c - The behaviour of the scattering amplitudes for \bar{e} - Li scattering at 300 eV.

Θ	f_{B1}	$R_{e1} f_{HEA}$	(2)	$R_e f_{W2}$	$R_{e2} f_{HEA}$	(2)	$I_m f_{HEA}$	(2)	f_{G3}
5	4.64	7.8139(-1)	1.1078(-1)	1.2676(-1)	1.3301	1.5077(-1)			
10	2.83	6.4417(-1)	7.0440(-2)	1.2294(-1)	5.8970(-1)	6.08(-1)			
20	1.02	4.8958(-1)	2.4227(-2)	1.2965(-2)	4.6944(-1)	4.81(-1)			
30	5.48(-1)	3.9597(-1)	1.0596(-2)	3.7990(-3)	3.4313(-1)	4.05(-1)			
40	3.57(-1)	3.1612(-1)	5.8628(-3)	1.1304(-3)	2.5890(-1)	3.67(-1)			
50	2.65(-1)	2.5114(-1)	3.7604(-3)	3.8000(-4)	2.0731(-1)	3.01(-1)			
60	2.13(-1)	2.0112(-1)	2.6530(-3)	1.2910(-4)	1.7357(-1)	2.87(-1)			
70	1.68(-1)	1.5498(-1)	2.0010(-3)	3.5225(-5)	1.4995(-1)	2.57(-1)			
80	1.42(-1)	1.3593(-1)	1.5841(-3)	1.5634(-5)	1.3256(-1)	2.31(-1)			
90	1.22(-1)	1.1535(-1)	1.3041(-3)	1.1180(-5)	1.1930(-1)	2.26(-1)			

Table : 4.13 : d - The behaviour of the scattering amplitudes for $\bar{e} - Li$ scattering at 400 eV.

Q	f_{B1}	$R_{e1} f_{HEA}$	(2)	$R_e f_{w2}$	$R_e f_{HEA}$	$R_{e2} f_{HEA}$	$I_m f_{HEA}$	(2)	$I_m f_{HEA}$	f_{G3}
5	4.36	6.5853(-1)	7.850(-2)	8.206(-2)	9.263(-1)	4.48(-1)				
10	2.37	5.2846(-1)	4.469(-2)	7.857(-2)	4.713(-1)	4.41(-1)				
20	8.08(-1)	3.9771(-1)	1.359(-3)	1.259(-2)	3.684(-1)	3.39(-1)				
30	4.46(-1)	3.0882(-1)	5.852(-3)	5.611(-3)	2.569(-1)	2.84(-1)				
40	4.26(-1)	2.3575(-1)	3.249(-3)	4.200(-3)	1.923(-1)	1.90(-1)				
50	2.49(-1)	1.8037(-1)	2.092(-3)	1.100(-3)	1.539(-1)	1.85(-1)				
60	1.70(-1)	1.4036(-1)	1.479(-3)	2.000(-4)	1.287(-1)	1.76(-1)				
70	1.48(-1)	1.1196(-1)	1.117(-3)	1.890(-4)	1.109(-1)	1.70(-1)				
80	1.19(-1)	9.1694(-2)	8.860(-4)	1.510(-4)	9.770(-2)	1.60(-1)				
90	9.46(-2)	7.7060(-2)	7.301(-4)	1.051(-4)	8.759(-2)	1.52(-1)				

FIG: 4.2

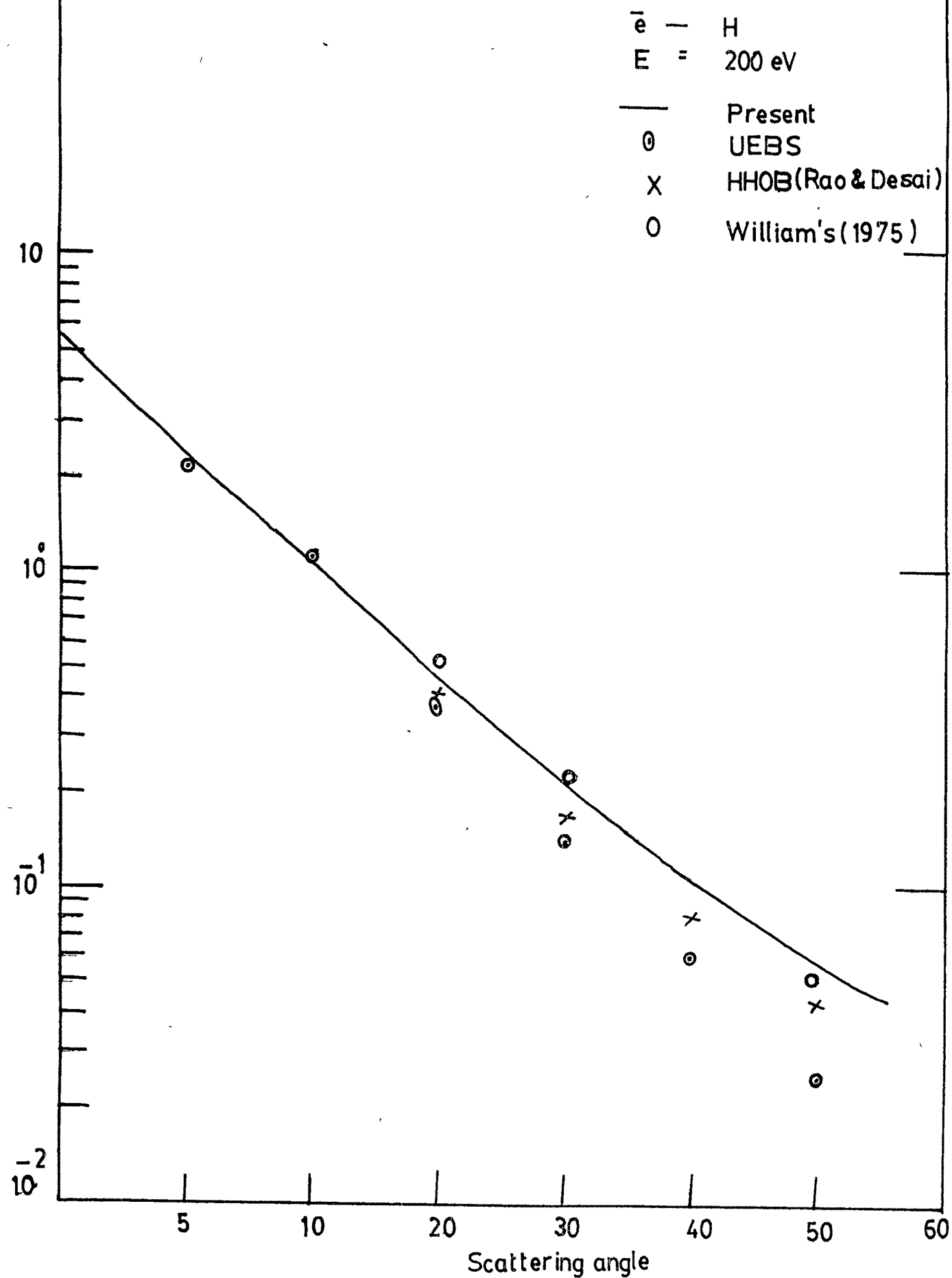


FIG: 4.3

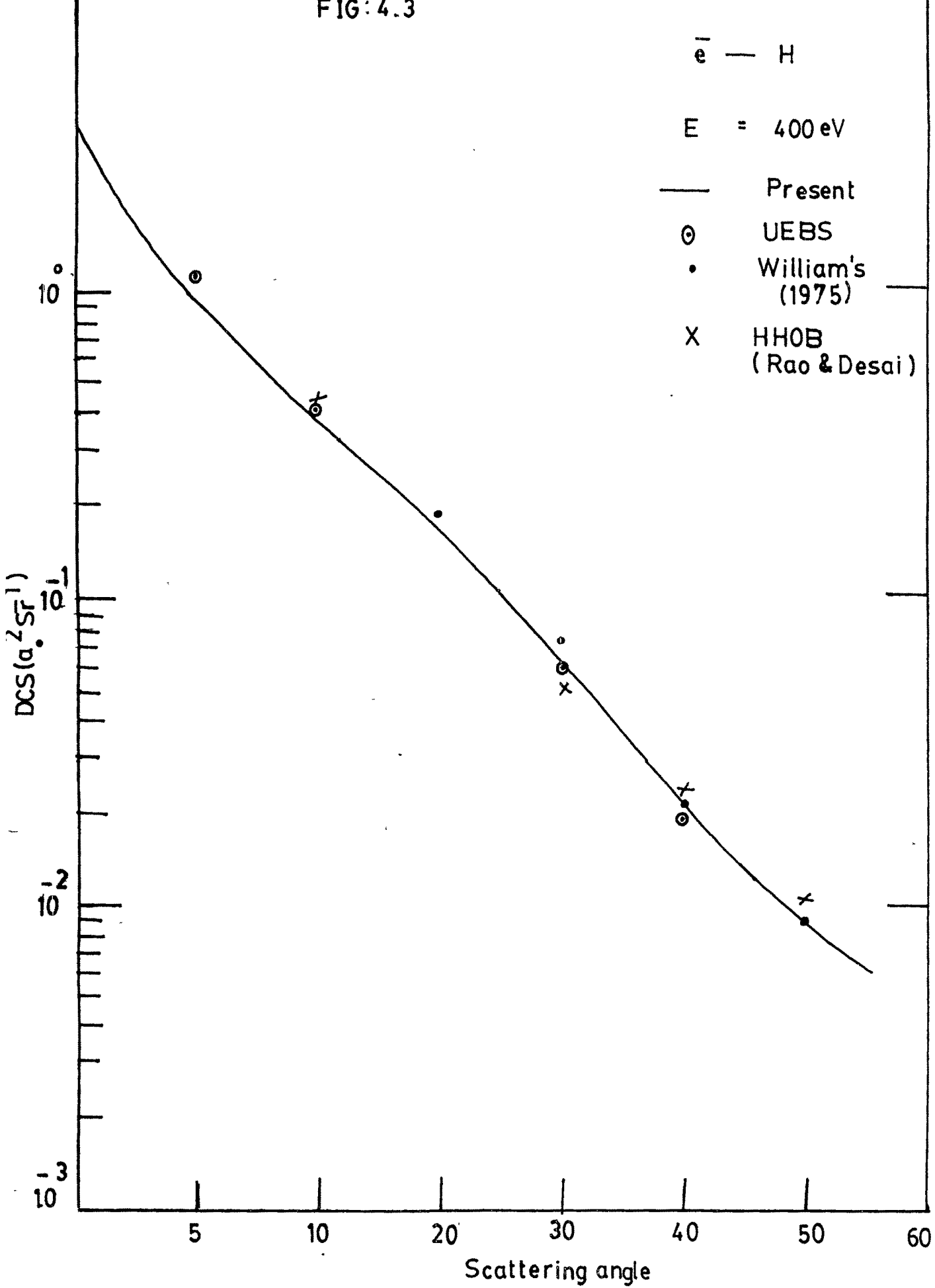


FIG: 4.4

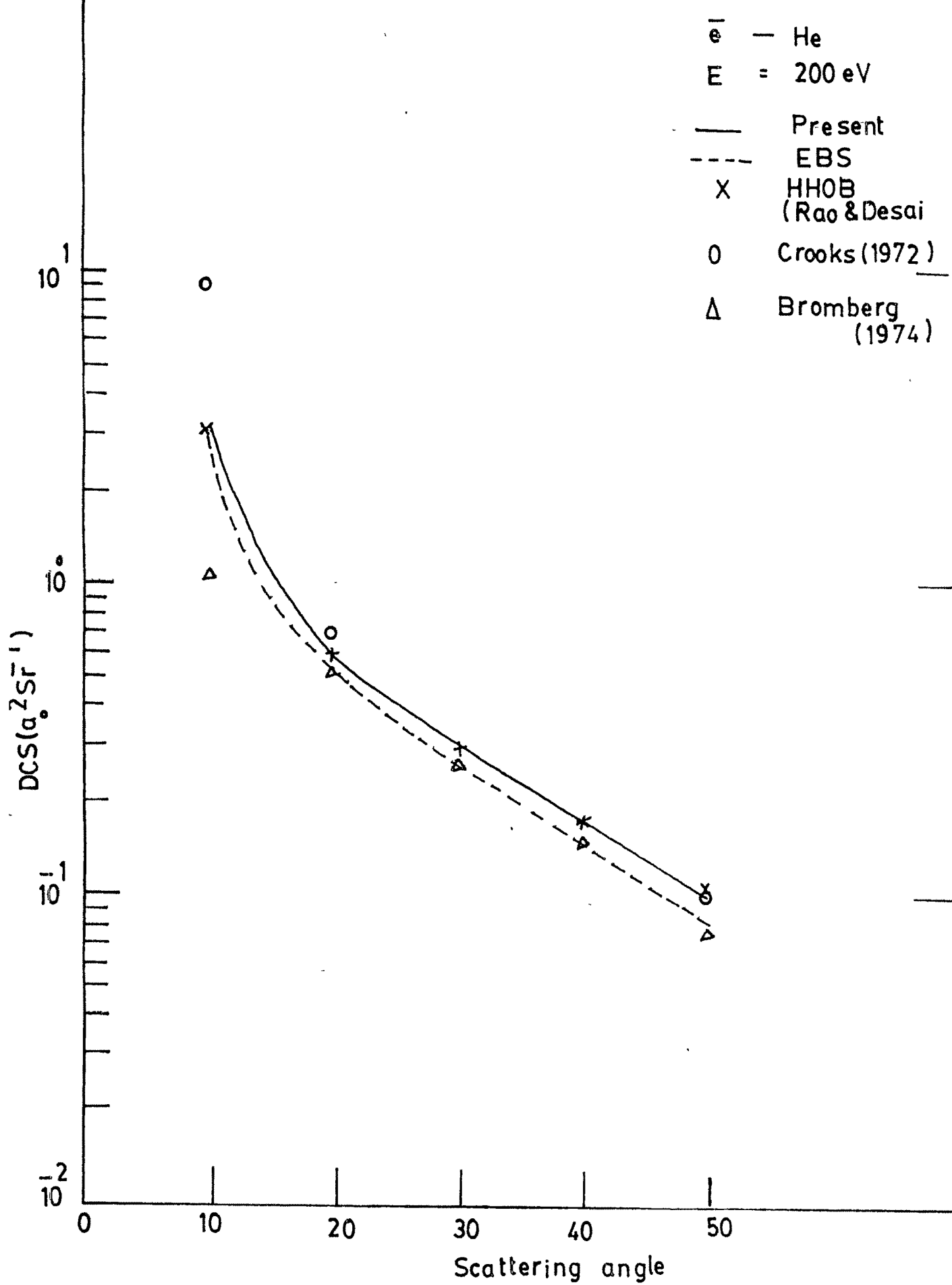


FIG: 4.5

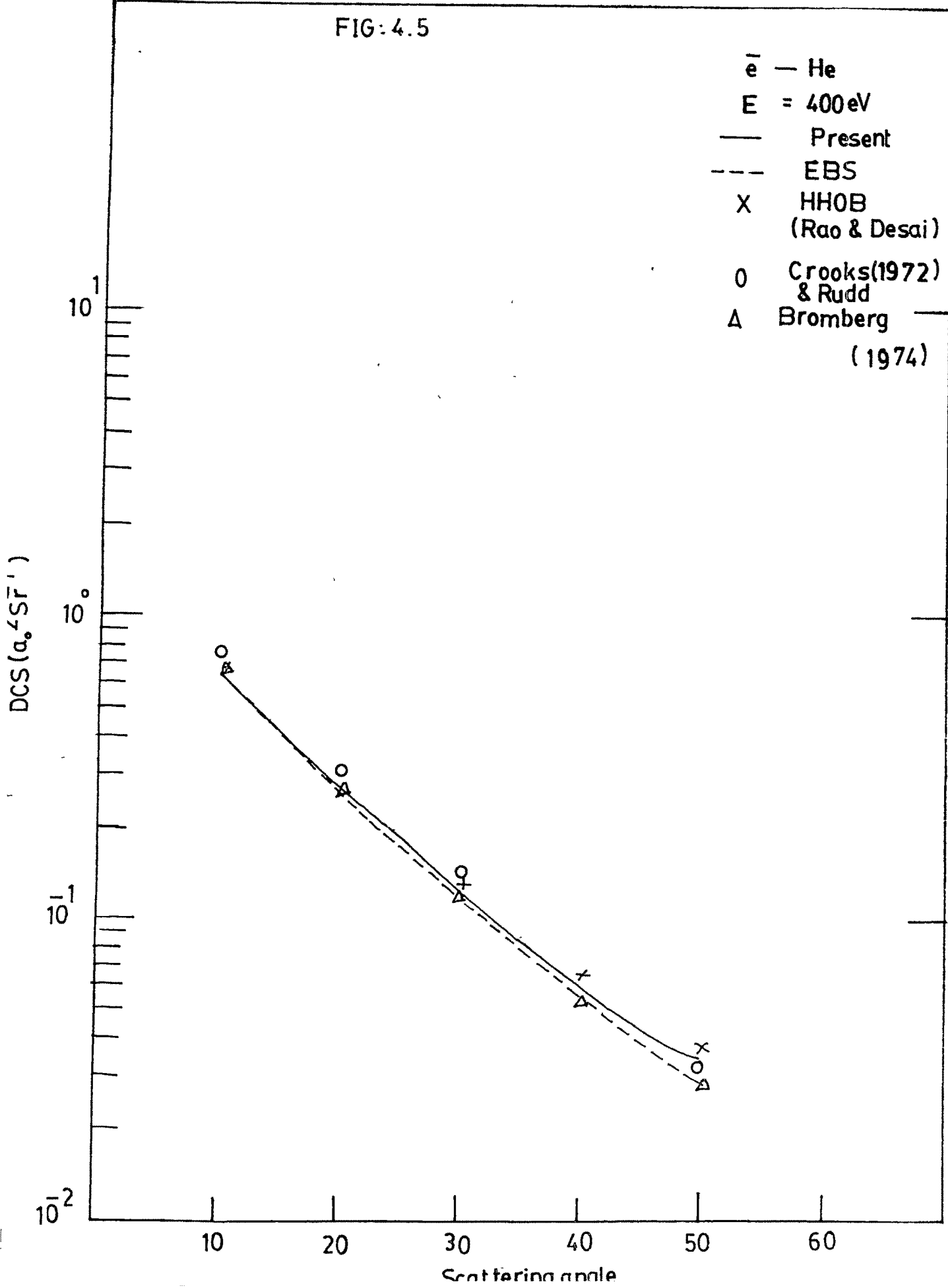


FIG: 4.6

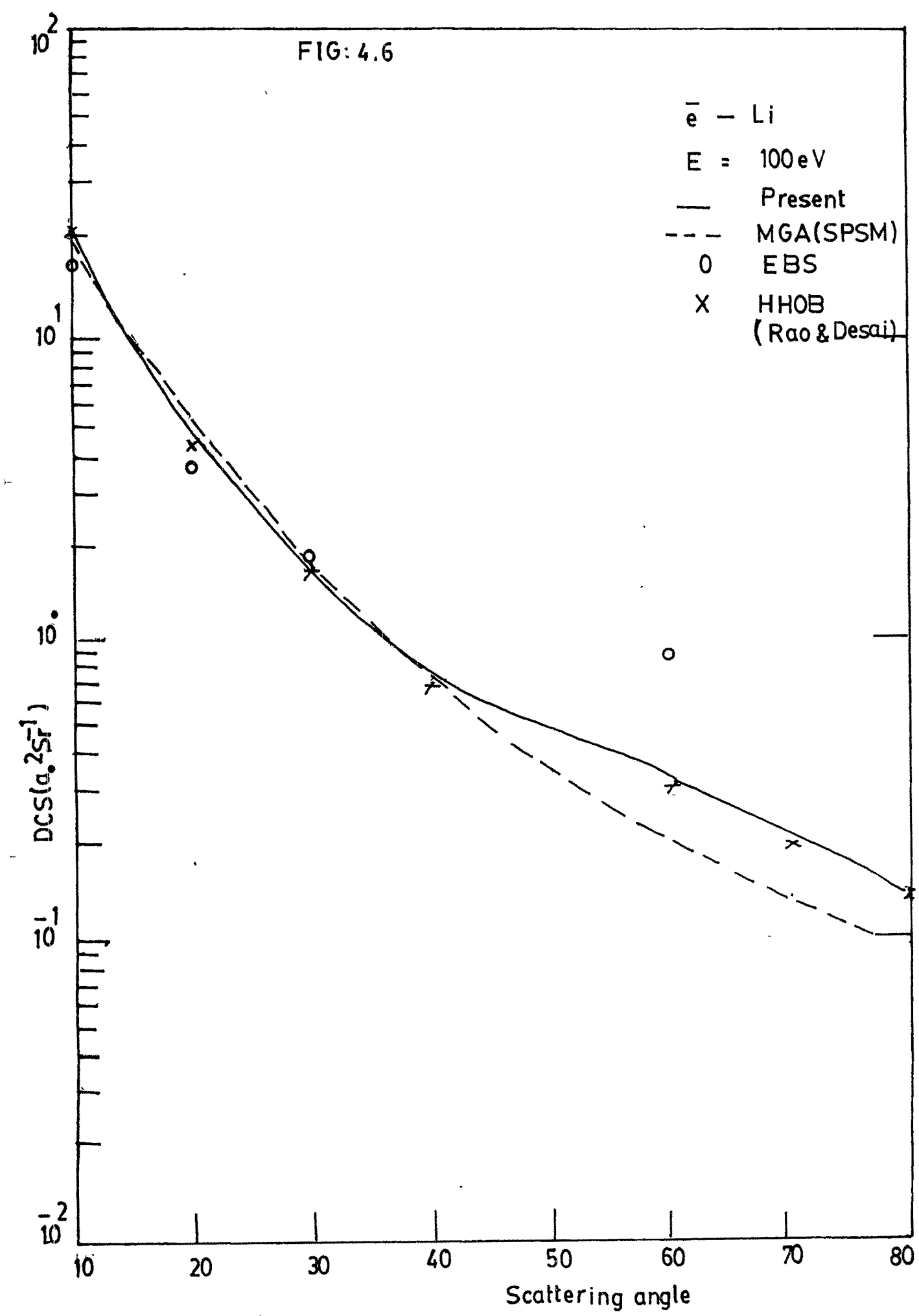


FIG:4.7

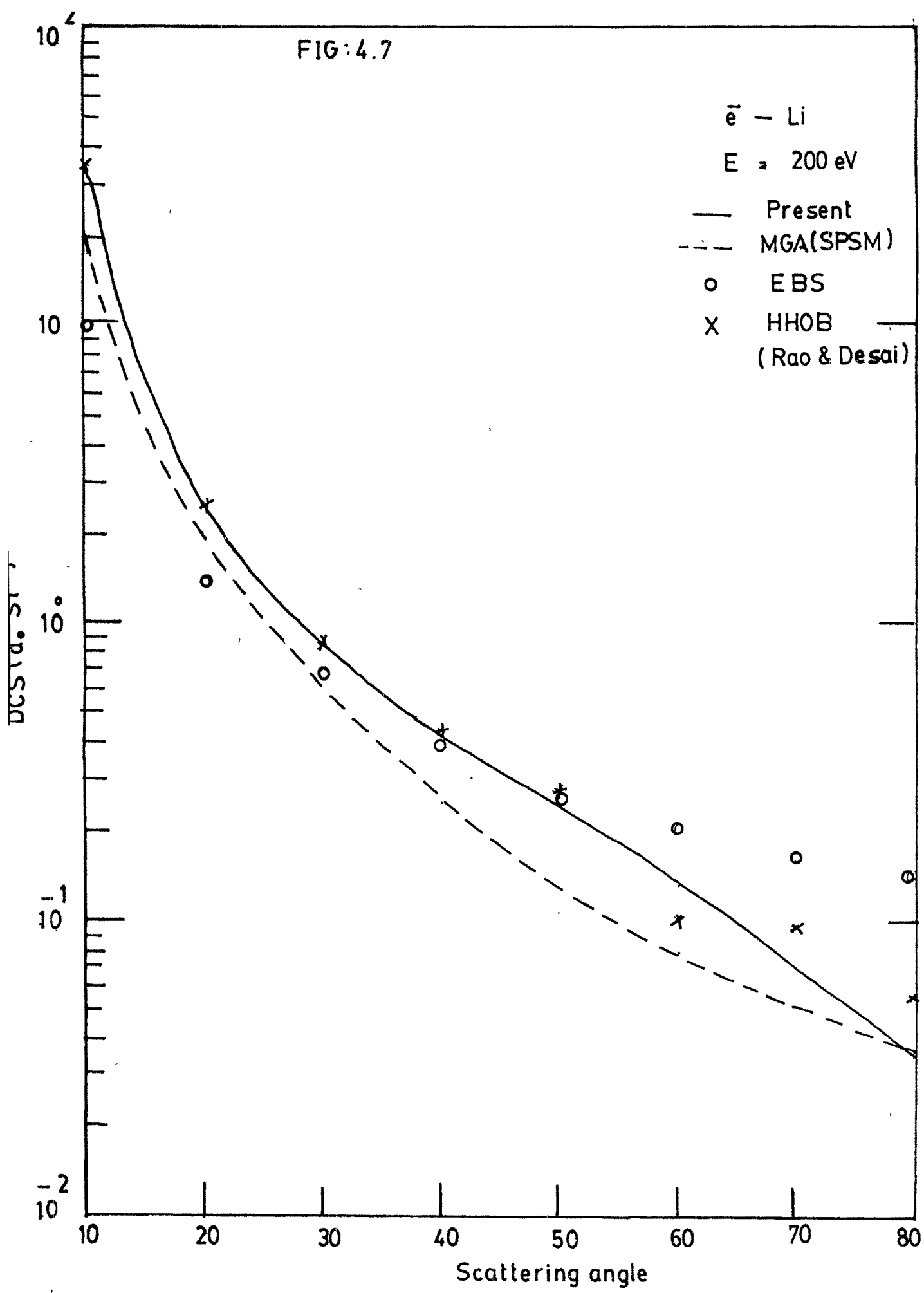


FIG:4.8

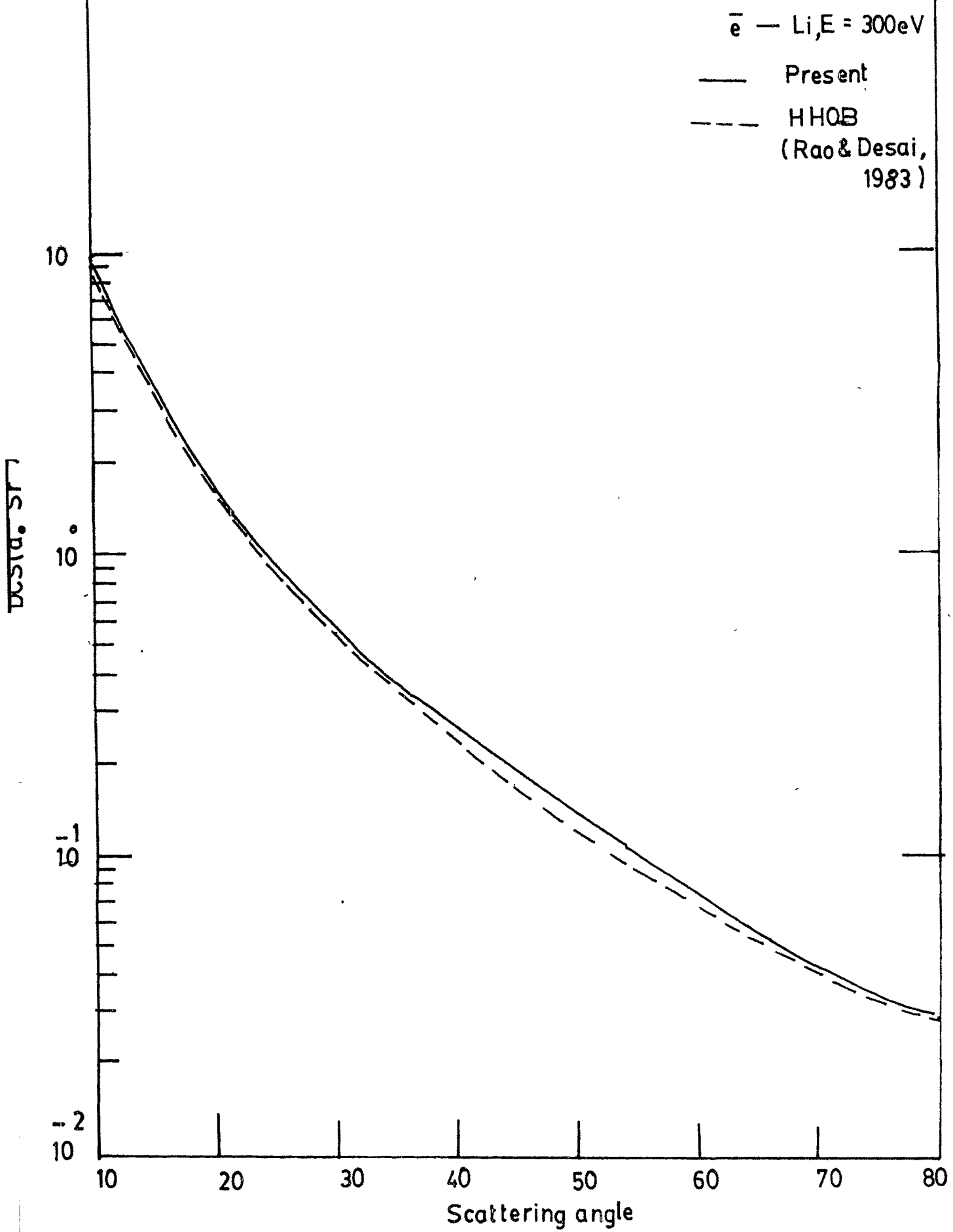


FIG: 4.9

